Supramolecular Explorations: Exhibiting the Extent of Extended Cationic Cyclophanes

Journal:	*Accounts of Chemical Research*
Manuscript ID	ar-2015-00495r.R1
Manuscript Type:	Article
Date Submitted by the Author:	07-Jan-2016
Complete List of Authors:	Dale, Edward; Northwestern University, Department of Chemistry Vermeulen, Nicolaas; Northwestern University, Department of Chemistry Juricek, Michal; University of Basel, Department of Chemistry Barnes, Jonathan; Massachusetts Institute of Technology, Chemistry Young, Ryan; Northwestern University, Chemistry Wasielewski, Michael; Northwestern University, Department of Chemistry Stoddart, J. Fraser; Northwestern University, Department of Chemistry

Supramolecular *Ex*plorations: *Ex*hibiting the *Ex*tent of *Ex*tended Cationic Cyclophanes

Edward J. Dale,[†] Nicolaas A. Vermeulen,[†] Michal Juríček,[§] Jonathan C. Barnes,[₪] Ryan M. Young,[⌂] Michael R. Wasielewski[⌂*] and J. Fraser Stoddart[†*]

[†]Department of Chemistry, Northwestern University, 2145 Sheridan Road, Evanston, Illinois 60208, United States

[§]Department of Chemistry, University of Basel, St. Johanns-Ring 19, 4056 Basel, Switzerland

[₪]Department of Chemistry, Massachusetts Institute of Technology, 77 Massachusetts Avenue, Cambridge, Massachusetts, 02139, United States

[⌂]Department of Chemistry and Argonne-Northwestern Solar Energy Research (ANSER) Center, 2145 Sheridan Road, Evanston, Illinois 60208, United States

■ CONSPECTUS

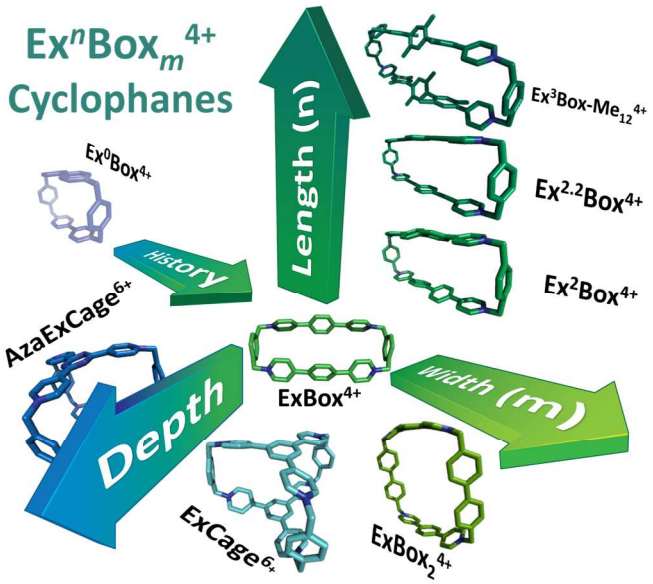

Acting as hosts, cationic cyclophanes, consisting of π-electron-poor bipyridinium units, are capable of entering into strong donor–acceptor interactions to form host–guest complexes with various guests when the size and electronic constitution are appropriately matched. A synthetic protocol has been developed which utilizes catalytic quantities of tetrabutylammonium iodide (TBAI) to make a wide variety of cationic pyridinium-based cyclophanes in a quick and easy manner. Members of this class of cationic cyclophanes with *box*-like geometries, dubbed **Ex^{n}Box$_{m}$$^{4+}$** for short, have been prepared by altering a number of variables — (i) ***n***, the number of "horizontal" *p*-phenylene spacers between adjoining pyridinium units, thus modulating the "length" of the cavity, (ii) ***m***, the number of "vertical" *p*-phenylene spacers to modulate the "width" of the cavity, and (iii) the aromatic linkers, namely 1,4-di- and 1,3,5-trisubstituted units in the construction of macrocycles (**ExBoxes**) and macrobicycles (**ExCages**), respectively.

This Account serves as an exploration of the properties that emerge from these structural modifications on the pyridinium-based hosts, coupled with a call for further investigation into the wealth of properties inherent in this class of compounds. By only varying the aforementioned components, the role of these cationic receptors cover ground that spans (i) synthetic methodology, (ii) extraction and sequestration, (iii) catalysis, (iv) molecular electronics, (v) physical organic chemistry, and (vi) supramolecular chemistry. **Ex^{1}Box^{4+}** — or simply **ExBox^{4+}** — has been shown to be a multipurpose receptor capable of binding a wide range of polycyclic

aromatic hydrocarbons (PAHs), while also being a suitable component in switchable mechanically interlocked molecules. Additionally, the electronic properties of some host–guest complexes allow for the development of artificial photosystems. $\mathbf{Ex^2Box^{4+}}$ boasts the ability to bind both π-electron-rich and -poor aromatic guests in different binding sites located within the same cavity. $\mathbf{ExBox_2^{4+}}$ forms complexes with C_{60} in which discrete arrays of aligned fullerenes result in single co-crystals, leading to improved material conductivities. When the substitution pattern of the $\mathbf{Ex^nBox^{4+}}$ series is changed to 1,3,5-trisubstituted benzenoid cores, the hexacationic *cage*-like compound, referred to as $\mathbf{ExCage^{6+}}$, exhibits different kinetics of complexation with guests of varying sizes — a veritable playground for physical organic chemists.

The organization of functionality with respect to structure becomes valuable as the number of analogues continues to grow. With each of these minor structural modifications, a wealth of properties emerge, begging the question as to what discoveries await and what properties will be realized with the continued exploration of this relatively neglected area of supramolecular chemistry based on this unique class of receptor molecules.

■ INTRODUCTION

The advent of chemistry beyond the molecule marked a departure from the preoccupation chemists have with covalent and strong coordinative bonds. Pedersen's discovery[1] of the crown ethers opened the way for synthetic chemists to design molecules that function as selective molecular receptors utilizing weak coordinative and noncovalent bonding interactions. His communication[2] and landmark paper,[3] both published in 1967, were followed by seminal contributions from Lehn[4,5] and Cram,[6] who introduced sequentially more complex receptors with the objective of expanding molecular recognition in a modern-day lock-and-key[7] sense. Their

early work in establishing supramolecular[8] and host–guest[9] chemistry, respectively, laid the foundations upon which macrocyclic receptors — cyclodextrins,[10,11] crown ethers,[3,12] calixarenes,[13,14] cucurbiturils,[15,16] porphyrins,[17,18] cyclophanes,[19,20] and pillararenes,[21,22] — have assumed a wide range of applications.

Tetracationic cyclophanes,[23] consisting of π-electron-deficient bipyridinium units, are capable of entering into donor–acceptor interactions with π-electron-rich guests to form either 1:1 or 1:2 complexes, depending on the size of the cyclophane's cavity. Cyclobis(paraquat-*p*-phenylene)[24] (**CBPQT**$^{4+}$) — one of the most ubiquitous tetracationic cyclophanes — plays a central role in the chemistry of mechanically interlocked molecules[25] (MIMs). This cyclophane is comprised of two π-electron-deficient 4,4′-bipyridinium units, connected end-to-end by *p*-xylylene linkers, creating a rigid inner cavity, suitable for the encapsulation of π-electron-rich substrates such as 1,5-dioxynaphthalene[26] and tetrathiafulvalene[27] derivatives. Under reducing conditions, the diradical, dicationic $\mathbf{Ex^0Box^{2(\bullet+)}}$ forms strong radical pairs with other viologen-based radicals.[28]

Recently, a synthetic protocol, which utilizes a modified Finklestein reaction with catalytic tetrabutylammonium iodide[29] (TBAI), was developed[30] to synthesize a wide variety of pyridinium-based cyclophanes. This class (**Figure 1**) of positively charged cyclophanes can be prepared (**Table 1**) by altering a number of variables — (i) ***n***, the number of "horizontal" *p*-phenylene spacers between adjoining pyridinium units, thus modulating the "length" of the cavity, (ii) ***m***, the number of "vertical" *p*-phenylene spacers to modulate the "width" of the cavity, and (iii) the aromatic linkers, namely 1,4-di- and 1,3,5-trisubstituted units in the construction of macrocycles[30–33] (**ExBoxes**) and macrobicycles[34,35] (**ExCages**), respectively. Here, we discuss the consequences of these constitutional changes on the complexation of neutral polycyclic aromatic hydrocarbons (PAHs) by this class of receptors. With each

modification, a wealth of properties emerge, begging the question as to what discoveries await their continued exploration.

■EXPANDING EX^0BOX^{4+} — IMPROVED SYNTHESIS

In order to investigate the properties of such a wide range of potential pyridinium-based receptors, we have developed a synthetic methodology[30] for the quick and efficient production of these compounds. Previously reported reaction conditions result in the generation of oligomers and byproducts that require multiple chromatographic and crystallization steps to obtain pure

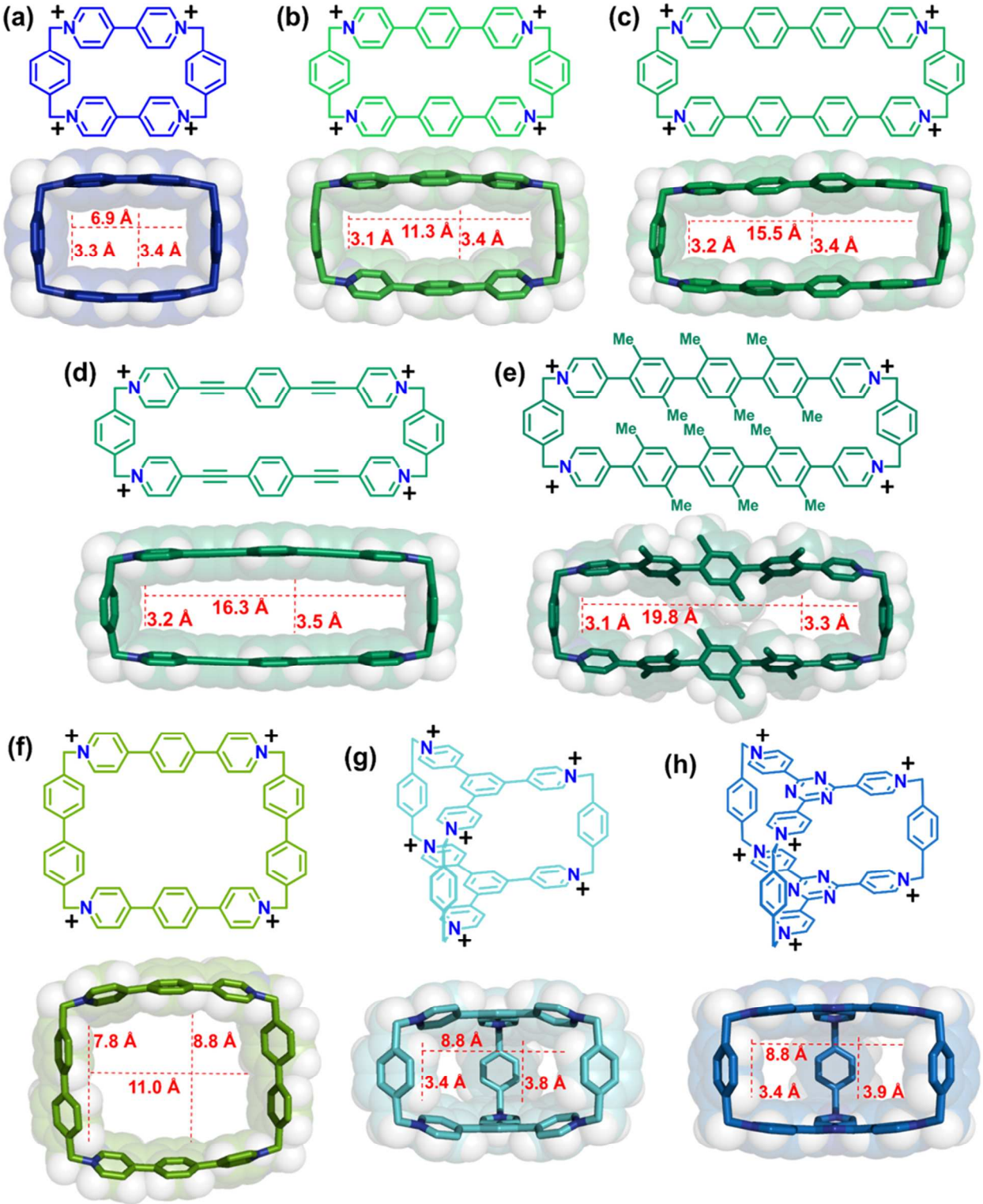

Figure 1. The structural formulas and dimensions of the binding cavity in the solid-state are shown for **(a) Ex^0Box^{4+}**, **(b) Ex^1Box^{4+}**, **(c) Ex^2Box^{4+}**, **(d) $Ex^{2.2}Box^{4+}$**, **(e) $Ex^3Box\text{-}Me_{12}^{4+}$**, **(f) $ExBox_2^{4+}$**, **(g) $ExCage^{6+}$**, and **(h) $AzaExCage^{6+}$**. The internal binding cavity distances are reported with respect to their van der Waals surfaces. Note that the colors used to represent the receptors have been chosen to match those employed in the original publications.

Table 1. Synthesis of $Ex^nBox_m^{4+}$ and $Ex^nCage_m^{6+}$ Variants.

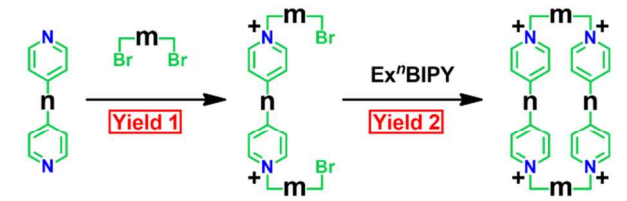

Ex^{n}BIPY Ex^{n}DB$_m$$^{2+}$ Ex^{n}Box$_m$$^{4+}$

Structure		Product	Yield 1	Yield 2
n	*m*		%	%
N/A		Ex^{0}Box$_1$$^{4+}$	70	20
		Ex^{1}Box$_1$$^{4+}$	92	66
		Ex^{2}Box$_1$$^{4+}$	72	37
		Ex$^{2.2}$Box$_1$$^{4+}$	93	29
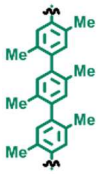		Ex^{3}Box$_1$-Me$_{12}$$^{4+}$	98	14
		Ex^{1}Box$_2$$^{4+}$	72	18

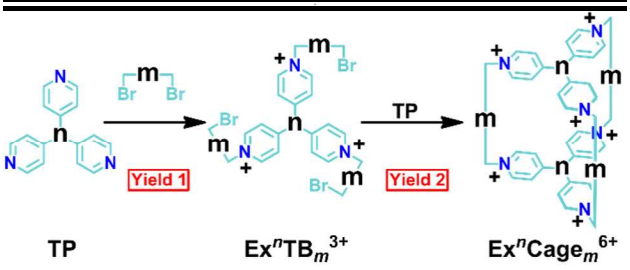

TP Ex^{n}TB$_m$$^{3+}$ Ex^{n}Cage$_m$$^{6+}$

Structure		Product	Yield 1	Yield 2
n	*m*		%	%
		Ex^{1}Cage$_1$$^{6+}$	75	45
		AzaEx^{1}Cage$_1$$^{6+}$	58	11

products. Generally, a template, which complicates purification, is added to the reaction mixture to facilitate intramolecular macrocyclization over intermolecular oligomerization. Finally, under high dilution, reaction times are generally long, *e.g.*, weeks. Using TBAI as a catalyst, along with increased temperatures and high-dilution techniques, tetracationic cyclophanes can be produced (**Table 1**) in good yields in short reaction times (*e.g.* days) without the need for chromatographic separations.

Templates,[36,37] catalyst, and temperature were all varied when exploring the synthesis of **ExBox**$^{4+}$ as a test case. The benefits of employing TBAI as a catalyst, along with increased reaction temperatures became evident. Previous reactions to form **ExBox**$^{4+}$ required[31] at least 14 days to progress to completion, yet after less than 3 days with 0.2 equiv of TBAI at 80 °C in MeCN, the starting materials were all consumed. Moreover, a template is not necessary and high yields — 66% using TBAI versus 42% reported[31] previously (templated) — were achieved. Since oligomeric products are suppressed in the presence of TBAI, even without using templates, the crude mixture does not require column chromatography. Two crystallizations are sufficient to yield pure compounds.

When the same synthetic procedure was applied to the synthesis of **CBPQT**$^{4+}$ (**Ex^{0}Box**$^{4+}$), the outcome was[30] production on the gram-scale without any need for chromatography. Furthermore, **Ex^{3}Box-Me$_{12}$**•4PF$_6$, whose synthesis had eluded us on account of its poor solubility and the lack of a suitable template, was obtained in 14% yield. With this new synthetic protocol in place, it becomes possible to make a wide selection (**Figure 1**) of positively charged cyclophanes.

■ The First Dimension — Binding of Planar PAHs

The geometries and electronic properties of the **Ex^{n}Box**$^{4+}$ cyclophanes give rise to the multiple cooperative noncovalent bonding forces responsible for their high binding affinities toward

PAHs. These forces include (1) π-donor–π-acceptor, (2) electrostatic ion–quadrupole, (3) edge-to-face CH···π interactions, (4) van der Waals (London dispersion) interactions, and (5) solvophobic forces. The π–π interactions arise because of proximity of the π-electron-rich PAHs to two sandwiching π-electron-deficient Ex^{n}BIPY^{2+} units, held rigidly apart at near-optimal π–π stacking distances. The association constants (K_a) for the **Ex^{n}Box^{4+}** cyclophanes towards a series of PAHs were determined[31,32] in the case of **ExBox^{4+}** and **Ex^{2}Box^{4+}**, by either ^{1}H NMR titration or isothermal titration calorimetry (ITC) in MeCN. In the case of **Ex^{3}Box-Me$_{12}$$^{4+}$**, the methyl substituents, introduced to increase solubility, interfere with the binding of PAHs inside its cavity.[30] In the original investigation,[31] 11 crystalline inclusion complexes of **ExBox^{4+}** with PAHs were subjected to X-ray diffraction (XRD) studies as well as to UV/Vis and NMR spectroscopies. It was discovered that the complexation of PAHs by **ExBox^{4+}** is associated with K_a values that increase (**Figure 2**) exponentially with the number of π-electrons in the PAHs.

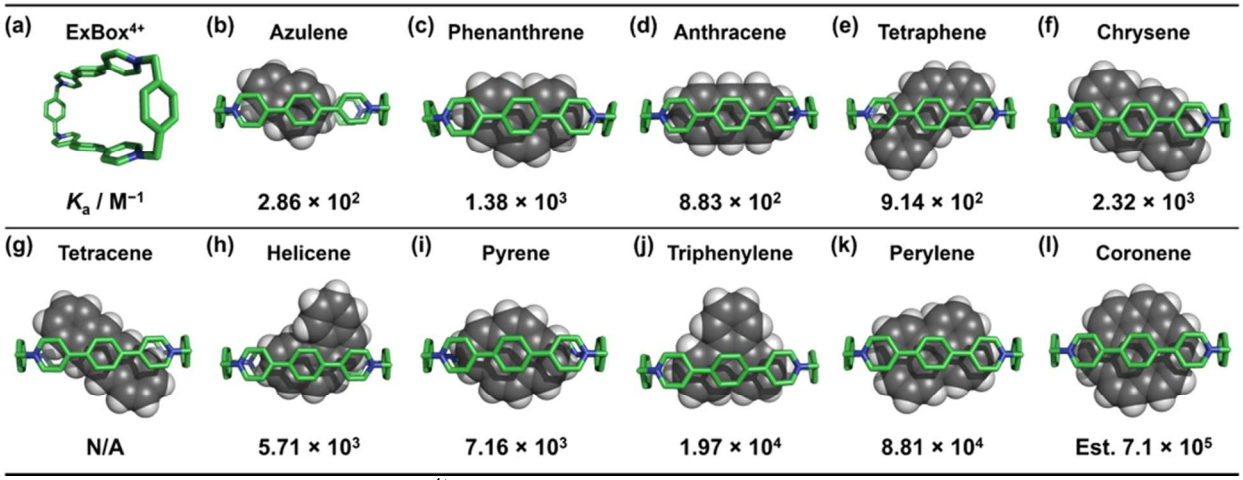

Figure 2. The internal cavity **(a)** of **ExBox^{4+}** and the solid-state superstructures and respective K_a values of the 1:1 complexes formed **(b-l)** with selected PAHs. Adapted with permission from reference 31. Copyright (2013) American Chemical Society.

The strengths of the π–π stacking interactions are reflected in the presence of charge-transfer (CT) bands in the UV/Vis spectra of the corresponding 1:1 inclusion complexes. The affinity of **ExBox^{4+}** to PAHs was also accorded some practical importance by extracting a crude oil sample from Saudi Arabia containing an unspecified array of aromatic compounds with an aqueous

solution of **ExBox**•4Cl.

The relative contributions of the electrostatic ion–quadrupole interactions and London dispersion forces were also assessed computationally.[38,39] Binding affinities for selected PAHs were compared inside $\mathbf{ExBox^{4+}}$ versus an all-carbon analog — which results in a neutral receptor with a geometry similar to that of $\mathbf{ExBox^{4+}}$, but removes the electrostatic component of the binding affinities. It was concluded that (i) the electrostatic component amounts to only 9.5–19.2% of the total binding enthalpy and (ii) the nonelectrostatic contributions dominate the binding of PAHs by $\mathbf{ExBox^{4+}}$. Since solvophobic effects[40] are often the main cause of errors when determining the binding enthalpies and free energies of complexation in solution, quantifying which forces dominate the binding of PAHs by $\mathbf{ExBox^{4+}}$ is not straightforward and requires further investigation.

■ Binding of Corannulene Inside $\mathbf{ExBox^{4+}}$

When the binding of corannulene — a bowl-shaped PAH — inside $\mathbf{ExBox^{4+}}$ was also investigated,[7,8] it was found that $\mathbf{ExBox^{4+}}$ possesses a sufficient degree of flexibility to accommodate this non-planar substrate. Corannulene is comprised of one central five-membered ring and five peripherally fused six-membered rings. It adopts a bowl-shaped geometry in its ground state and undergoes[41] a bowl-to-bowl inversion process through a planar transition state with an energy barrier of 11.5 kcal mol^{-1}. The bowl depth of corannulene is ~4.1 Å in van der Waals terms and is thus too tall to fit inside $\mathbf{ExBox^{4+}}$. In order for $\mathbf{ExBox^{4+}}$ to accommodate corannulene, both the receptor and substrate undergo conformational changes where $\mathbf{ExBox^{4+}}$ increases its width from 3.5 to 4.3 Å and corannulene decreases its bowl depth from 4.1 to 4.0 Å, as observed in the solid state. This "induced fit", however, comes with a cost in energy. The K_a

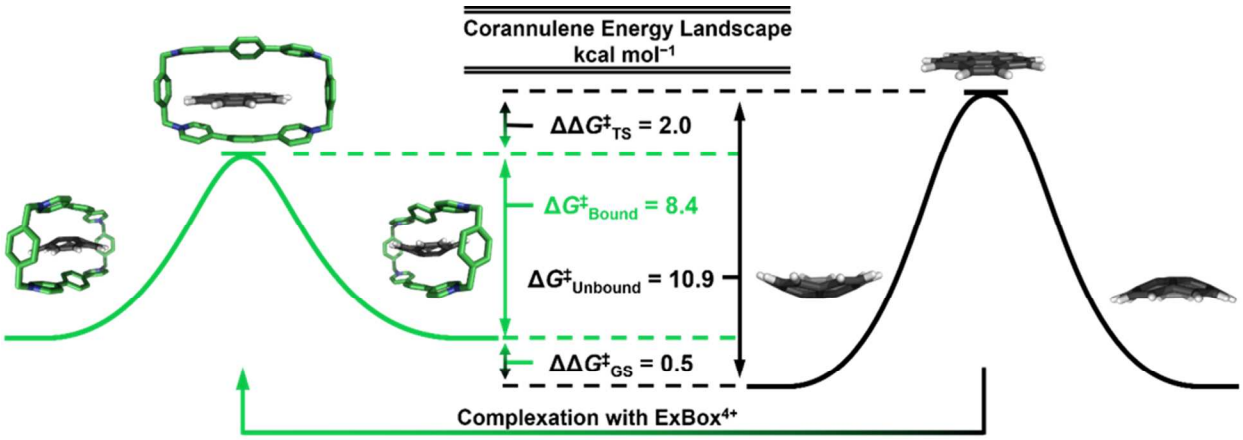

Figure 3. In good agreement with the experimental data showing a ~2 kcal mol^{-1} decrease in the inversion barrier of corannulene within **ExBox**$^{4+}$, DFT calculations reveal both ground-state destabilization and transition-state stabilization. Adapted with permission from reference 42. Copyright (2014) Nature Publishing Group.

value for binding of corannulene to **ExBox**$^{4+}$ in MeCN was found to be 6.45 × 10^3 M^{-1}, while that for perylene was found to be 8.80 × 10^4 M^{-1}. As both these PAHs possess the same number of π-electrons — and their binding affinity is expected[31] to be similar — the energy "loss" (~2 kcal mol^{-1}) in the case of corannulene can be attributed to the structural perturbation, resulting in strained molecules. It was shown[42] that this energy "stored" in the form of strain in **ExBox**$^{4+}$ forces corannulene to adopt a flatter conformation inside **ExBox**$^{4+}$, which effectively decreases the energy barrier by ~2 kcal mol^{-1} for the bowl-to-bowl inversion process in corannulene. Consequently, **ExBox**$^{4+}$ catalyzes the bowl-to-bowl inversion process of corannulene by distorting the bowl-shaped ground state and stabilizing the planar transition state of corannulene, by means of an induced-fit mechanism,[43] as demonstrated by the ~2 kcal mol^{-1} decrease in the inversion barrier by dynamic ^{1}H NMR spectroscopy, supported (**Figure 3**) by *in silico* modeling.

■ Binding Affinity of Ex^{2}Box^{4+}

The constitution of **Ex^{2}Box**$^{4+}$ can be considered to be extended[32] by one additional phenylene ring in its bipyridinium units when compared with that of **ExBox**$^{4+}$. This extension, which results in a longer cavity with size of 18.9 Å, allows substrates to be as long as 15.5 Å taking into account van der Waals radii. The additional length introduced between pyridinium units leads to

a less uniform distribution of electron density inside $\mathbf{Ex^2Box^{4+}}$ (**Figure 4a**), rendering it possible to match the electron configuration of a substrate with that of the receptor. The positive charges are located in the corners of the cavity of $\mathbf{Ex^2Box^{4+}}$, making them relatively electron-deficient, while the central biphenylene unit is electron-rich in comparison. A significant difference in

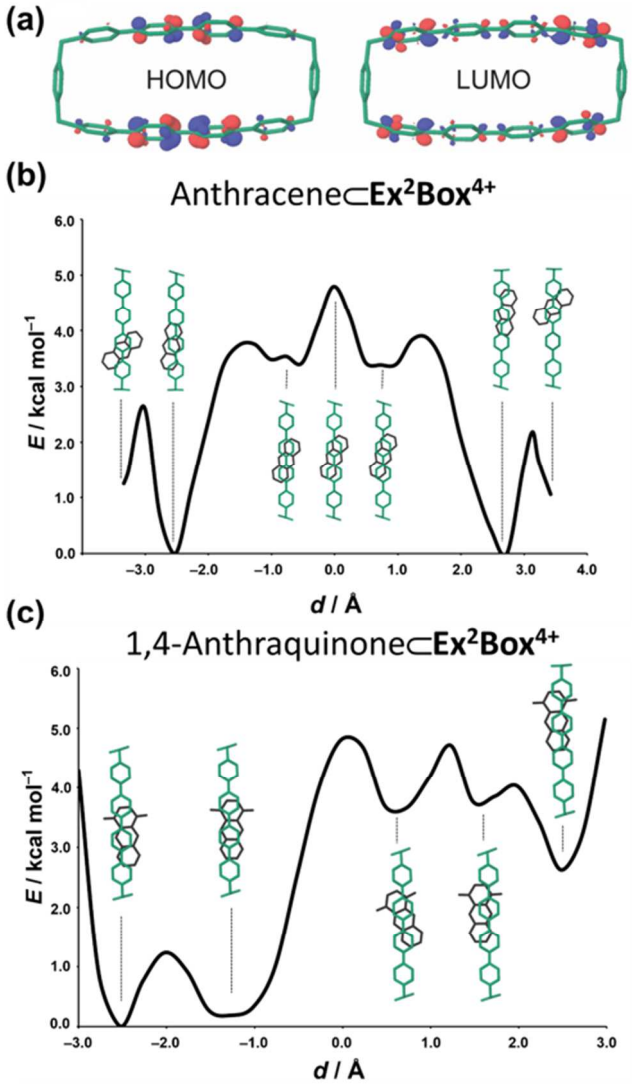

Figure 4. The computed (a) HOMO (left) and LUMO (right) of $\mathbf{Ex^2Box^{4+}}$. The optimized superstructures of the 1:1 complexes of (b) anthracene⊂$\mathbf{Ex^2Box^{4+}}$ and (c) 1,4-anthraquinone⊂$\mathbf{Ex^2Box^{4+}}$ and relative energies (*E*) were explored, resulting in an energy profile displaying the complementarity between the π-electron-rich and π-electron-poor portions of the receptor and substrates. Adapted with permission from reference 32. Copyright (2013) American Chemical Society.

binding affinities to PAHs was observed[1,2] between $\mathbf{ExBox^{4+}}$ and $\mathbf{Ex^2Box^{4+}}$. The shorter PAHs, anthracene and pyrene, are fully aligned (XRD, ^{1}H NMR) inside $\mathbf{ExBox^{4+}}$, while in $\mathbf{Ex^2Box^{4+}}$ they reside (XRD) at one end of the cavity. As a result, the binding affinity of anthracene and

pyrene is weaker in **Ex^{2}Box^{4+}** compared with the K_a values for **ExBox^{4+}**. This decrease in binding affinities is most likely the result of the fact that the favorable interactions, which contribute to binding only at one end of the cavity, are less pronounced. On the contrary, the binding affinities of longer acenes — namely, tetraphene and chrysene — are stronger in the case of **Ex^{2}Box^{4+}**, where the substrates can fully align (XRD), compared with those in **ExBox^{4+}**, where the substrates protrude from the cavity and hence fail to maximize their London dispersion interactions with the interior of **ExBox^{4+}**.

Calculations based on density functional theory (DFT) were performed on the complex of **Ex^{2}Box^{4+}** with anthracene in MeCN. The anthracene substrate was moved (**Figure 4b**) a distance (d / Å) along the internal cavity, revealing two distinct energetic minima. The first local minimum corresponds to the co-conformation, where the center of the anthracene resides as close as possible to the pyridinium rings at one end and is rotated by ~45° with respect to the long axis of **Ex^{2}Box^{4+}**, in agreement with the solid state. As the anthracene is moved towards the center, a second global minimum is observed, when the molecule is fully aligned inside **Ex^{2}Box^{4+}** and in close contact with the *p*-xylylene ring at one end. The global maximum is located when the substrate is aligned in the center of the cavity, where the favorable interactions are minimized.

In order to assess the binding of a π-electron-poor substrate within **Ex^{2}Box^{4+}**, the relative energetics for binding of 1,4-anthraquinone (**1,4-AQ**) inside **Ex^{2}Box^{4+}** were investigated (**Figure 4c**) by DFT calculations in a manner similar to that for anthracene, revealing that the global minimum corresponds to a co-conformation where the electron-rich portion of the substrate is closer to the pyridinium rings and the electron-poor portion closer to the center of the cavity. In the solid-state superstructure of the complex, **1,4-AQ** is positioned at one end, in agreement with

the prediction from calculations. 9,10-Anthraquinone was also investigated, resulting in a calculated minimum where the substrate resides in the center of the cavity, in agreement with complementary electronic configurations.

■ THE SECOND DIMENSION — EXBOX$_2^{4+}$

While most of the research on **ExBox**$^{4+}$ has exploited the near-optimal π–π stacking distance in order to bind planar aromatics, the case of the bowl-shaped corannulene encouraged us to extend the receptor in the ***m*** dimension. In an effort to encapsulate two planar substrates cofacially, or a single larger substrate, a pair of *p*-phenylene rings was introduced into each *p*-xylylene unit bridging the extended viologen units. This modification more than doubles the width of the cavity from 3.4 to 8.8 Å, when considering its van der Waals distances, compared to those in **ExBox**$^{4+}$, yielding[33] **ExBox$_2^{4+}$** (**Figure 5a**, top). In extending the **Ex^{n}Box$_m^{4+}$** series in the ***m*** dimension, the versatility in forming complexes becomes visible in the ability of **ExBox$_2^{4+}$** to accommodate large spherical aromatic substrates, such as C_{60}. It is important to note that the formation of C_{60}⊂**ExBox$_2^{4+}$** is another example of an induced-fit mechanism where, in the solid-state superstructure (**Figure 5a**, bottom) of the inclusion complex, the widest point in the ***m*** dimension of **ExBox$_2^{4+}$** measures 9.8 Å — that is, 1.0 Å wider than in its unbound state — while its length in the ***n*** dimension shortens simultaneously from 11.0 to 10.2 Å. Moreover, the complexation of C_{60} by **ExBox$_2^{4+}$** results (**Figure 5b**) in the long-range packing of C_{60} wherein each inclusion complex is in close van der Waals contact with a neighboring fullerene. The solid-state superstructure illustrates how the cyclophanes pack alongside each other, resulting in

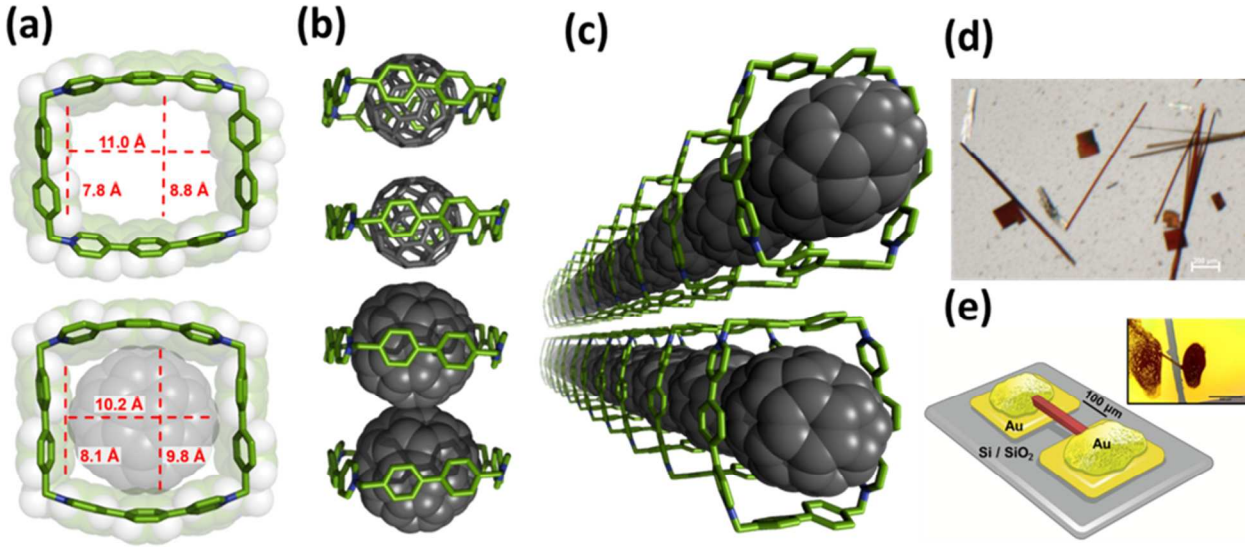

Figure 5. The solid-state (super)structures **(a)** of $\mathbf{ExBox_2}^{4+}$ (top) and $C_{60}\subset\mathbf{ExBox_2}^{4+}$ (bottom) are shown. The packing (b) of the superstructure displays the C_{60} molecules aligned within the cyclophane and (c) forms infinite channels of segregated arrays of C_{60}. The crystallization of $C_{60}\subset\mathbf{ExBox_2}\bullet 6PF_6$ results in (d) needle-like single crystals. A suitable crystal was mounted (e) on a gold surface on a Si/SiO_2 wafer using gold paste and the conductivity measured. Adapted with permission from reference 33. Copyright (2015) American Chemical Society.

continuous linear arrays of C_{60} that propagate (**Figure 5c**) the entire length of the crystal. This type of linear propagation is relatively uncommon in the supramolecular chemistry of unfunctionalized C_{60} molecules, although other examples are known.[44–46] Since C_{60} generally serves as an electron acceptor in most complexes,[47] the solution-phase binding between C_{60} and $\mathbf{ExBox_2}^{4+}$ was measured using ITC, revealed a modest K_a value of 2.5×10^3 M^{-1} in a DMF/PhMe (1:1) solution. Moreover, the thermodynamic parameters demonstrated that the formation of $C_{60}\subset\mathbf{ExBox_2}^{4+}$ reflects a favorable process ($\Delta G = -4.6$ kcal mol^{-1}) that is solvophobic in nature ($\Delta S = 23.9$ cal mol^{-1} K^{-1}), offsetting the unfavorable $\Delta H = 2.6$ kcal mol^{-1}.

In order to illustrate how the linear arrangement of C_{60} molecules could be advantageous from a device perspective, the bulk electrical conductivity of single crystals of $C_{60}\subset\mathbf{ExBox_2}^{4+}$ were measured and compared to that of single crystals consisting of $\mathbf{ExBox_2}^{4+}$ without C_{60}. The orientation of arrays of C_{60} were shown to coincide with the long-axis of the needle-like crystals by indexing the crystal with the unit cell obtained by XRD. The device was constructed (**Figure 6e**) by securing a $C_{60}\subset\mathbf{ExBox_2}^{4+}$ crystal between gold electrodes on a Si/SiO_2 wafer. The

electrical conductivity measured in this experiment was found to be 5.83×10^{-7} S cm^{-1}. When a similar device was constructed using single crystals comprised only of "empty" **ExBox$_2^{4+}$**, the electrical conductivity was found to be 1.20×10^{-9} S cm^{-1} — nearly 2.5 orders of magnitude lower than when C_{60} is present. These proof-of-concept experiments lay the foundation for future forays into materials science using other carbon allotropes in combination with the **Ex^{n}Box$_m^{4+}$** cyclophanes.

■ THE THIRD DIMENSION — EXCAGE^{6+}

By altering the substitution pattern from 1,4-di- to 1,3,5-trisubstituted benzenoid cores, the geometries of these "two-dimensional" box-like tetracationic cyclophanes change to that of a "three-dimensional" cage — namely **ExCage^{6+}** — with a trigonal geometry. **ExCage^{6+}** is

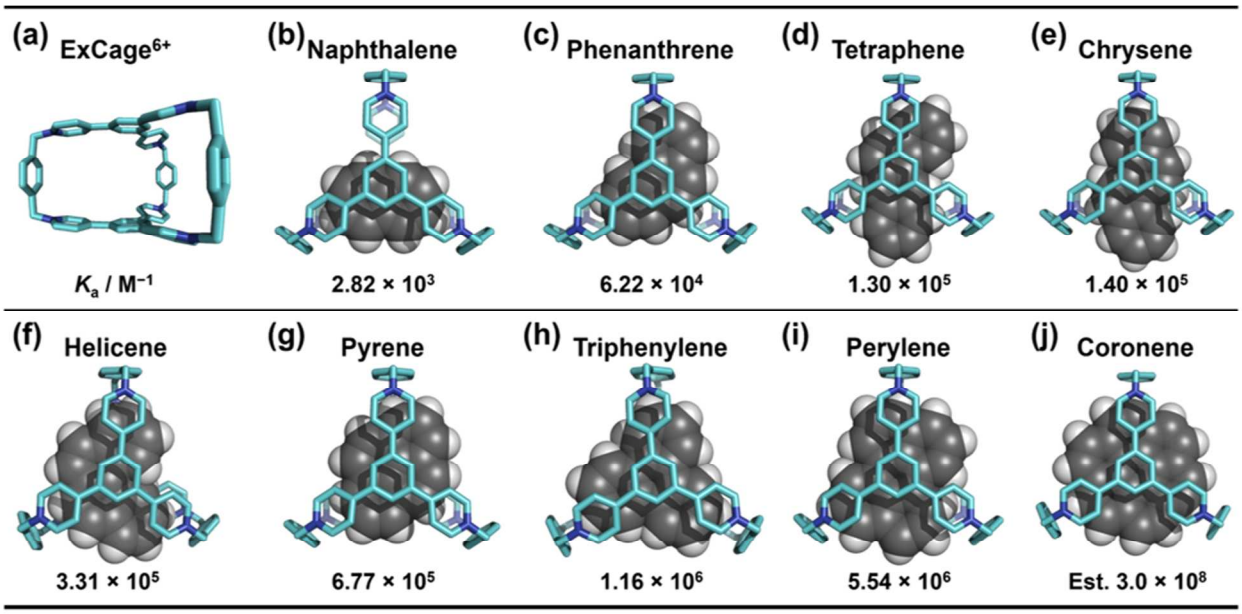

Figure 6. The internal cavity (a) of **ExCage^{6+}** and the 1:1 complexes formed **(b-j)** with selected PAHs and respective K_a values. Adapted with permission from reference 34. Copyright (2014) American Chemical Society.

comprised of a total of six π-electron deficient pyridinium units, resulting in strong donor–acceptor interactions with π-electron-rich PAHs, yielding a substantial increase in the binding affinities when compared to its **ExBox^{4+}** progenitor, allowing even naphthalene — one of the simplest PAHs — to enter into a strong complexation. The K_a values and thermodynamic

parameters between **ExCage**$^{6+}$ and eight PAHs were measured (**Figure 6**) by ITC in MeCN. Alternatively, another receptor, **AzaExCage**$^{6+}$, with a central triazine ring was synthesized.[35] With the relatively more electron-poor cavity, **AzaExCage**$^{6+}$ proved superior in binding PAHs compared to **ExCage**$^{6+}$ when using a large, non-coordinating counterion. In exploring the thermodynamic parameters (**Table 2**) of **ExCage**$^{6+}$, in conjunction with the solid-state structures, inclusion complexes appear to fall into three categories. Well-ordered complexes (**Table 2, red rectangle**) interact with all three pyridinium binding pockets simultaneously, resulting in a relatively large enthalpic stabilization that overcomes a substantial entropic penalty. Less well-ordered complexes (**Table 2, green rectangle**) interact with only two binding pockets at any one time, resulting in lower enthalpic and entropic contributions. Notably, **ExCage**$^{4+}$ binds naphthalene strongly (**Table 2, purple rectangle**), and is unique insofar as the binding is both enthalpically and entropically favorable. The solid-state superstructure indicates that, although

Table 2: Association Constants, Thermodynamic Parameters, and Comparative Free Energies of ExCage^{6+} and ExBox^{4+}

		ExCage•6PF_6 / MeCN / 298 K				**ExBox**•4PF_6 / MeCN / 298 K		
Guest	**π e$^-$**	**K_a (10^3 M^{-1})**	**ΔH (kcal mol^{-1})**	**ΔS (cal mol^{-1} K^{-1})**	**ΔG^0 (kcal mol^{-1})**	**K_a (10^3 M^{-1})**	**ΔG^0 (kcal mol^{-1})**	**$\Delta\Delta G^0$ (kcal mol^{-1})**
Naphthalene	10	2.82	−3.02	+5.60	−4.70	N/A	N/A	N/A
Phenanthrene	14	62.2	−9.07	−8.49	−6.54	0.88	−4.01	2.52
Tetraphene	18	130	−9.53	−8.78	−6.97	0.91	−4.03	2.94
Chrysene	18	140	−8.93	−6.42	−7.02	2.30	−4.58	2.43
Pyrene	16	677	−10.8	−9.10	−7.95	7.20	−5.26	2.69
Helicene	18	331	−12.5	−16.8	−7.53	5.71	−5.12	2.40
Triphenylene	18	1160	−13.4	−16.5	−8.27	19.7	−5.86	2.41
Perylene	20	5540	−13.1	−12.9	−9.19	88.1	−6.74	2.45
Coronene [a]	24	30000 [b]	N/A	N/A	N/A	700 [b]	N/A	N/A

[a] The binding constant for coronene could not be obtained on account of its insolubility in MeCN. [b] The K_a value for coronene is estimated based on a linear regression of the binding constants plotted against the number of π-electrons in naphthalene, phenanthrene, pyrene, triphenylene ,and perylene. Adapted with permission from reference 34. Copyright (2014) American Chemical Society.

naphthalene can access only two of the three binding and pockets, it exists with an included MeCN molecule as a highly disordered "ternary complex". The favorable entropy of binding

between **ExCage**$^{6+}$ and naphthalene comes as no surprise with a volume occupancy (**Figure 7)** of 53%, and stands in good agreement with Rebek's 55% rule.[48] The remaining substrates, which

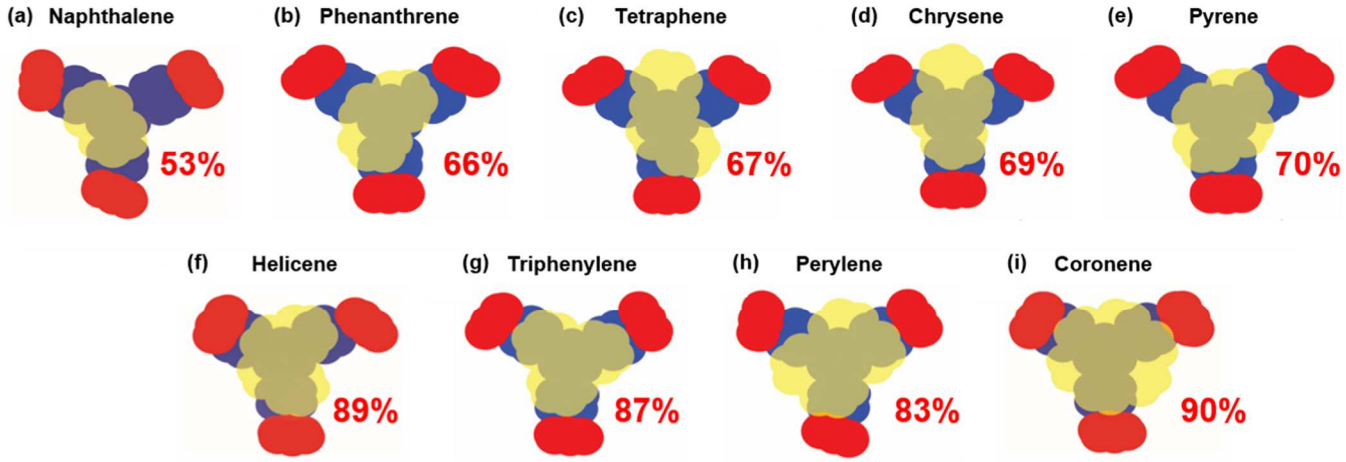

Figure 7. A surface-area overlap model used for the calculation of the percent volume occupancy. The PAH and **ExCage**$^{6+}$ were colored to show the non-binding phenylene units (red), the binding cavity (blue), and the area of the guest (light yellow). Adapted with permission from reference 34. Copyright (2014) American Chemical Society.

all occupy a significantly larger portion of the receptor — ranging from 66−90% — form much stronger complexes on account of the ever-increasing degree of molecular recognition in **ExCage**$^{6+}$, where enthalpy plays the dominating role.

In the cases of both **ExBox**$^{4+}$ and **ExCage**$^{6+}$, a linear trend on a logarithmic scale of the association constants versus π-electron count is observed (**Figure 8**), with aberrations observed in the cases of tetraphene and chrysene, on account of their elongated constitutions not being complementary with the binding cavity of **ExCage**$^{6+}$, and helicene, where the non-planarity limits the interaction with the pyridinium binding pockets. When the differences (*i.e.*, $\Delta\Delta G^0$) in ΔG^0 values on binding substrates are compared for **ExCage**$^{6+}$ and **ExBox**$^{4+}$, the former exhibits an average of −2.55 kcal mol^{-1} greater free energy of binding — a quantitative expression of the macrobicyclic effect. In diverging from the "two-dimensional" **ExBox**$^{4+}$ to the trigonal disposition of **ExCage**$^{6+}$, a structure is (**Figure 9a**) generated in which the three apertures are smaller than the binding cavity itself. A large substrate such as coronene will, therefore, experience (**Figure 9b**) a barrier to complexation based upon steric effects associated with the

bridging *p*-xylylene links. Cram coined[49] (**Figure 9c**) the terms *intrinsic binding* and *constrictive binding* corresponding to the free energy of complexation (ΔG^0) and the free energy of activation

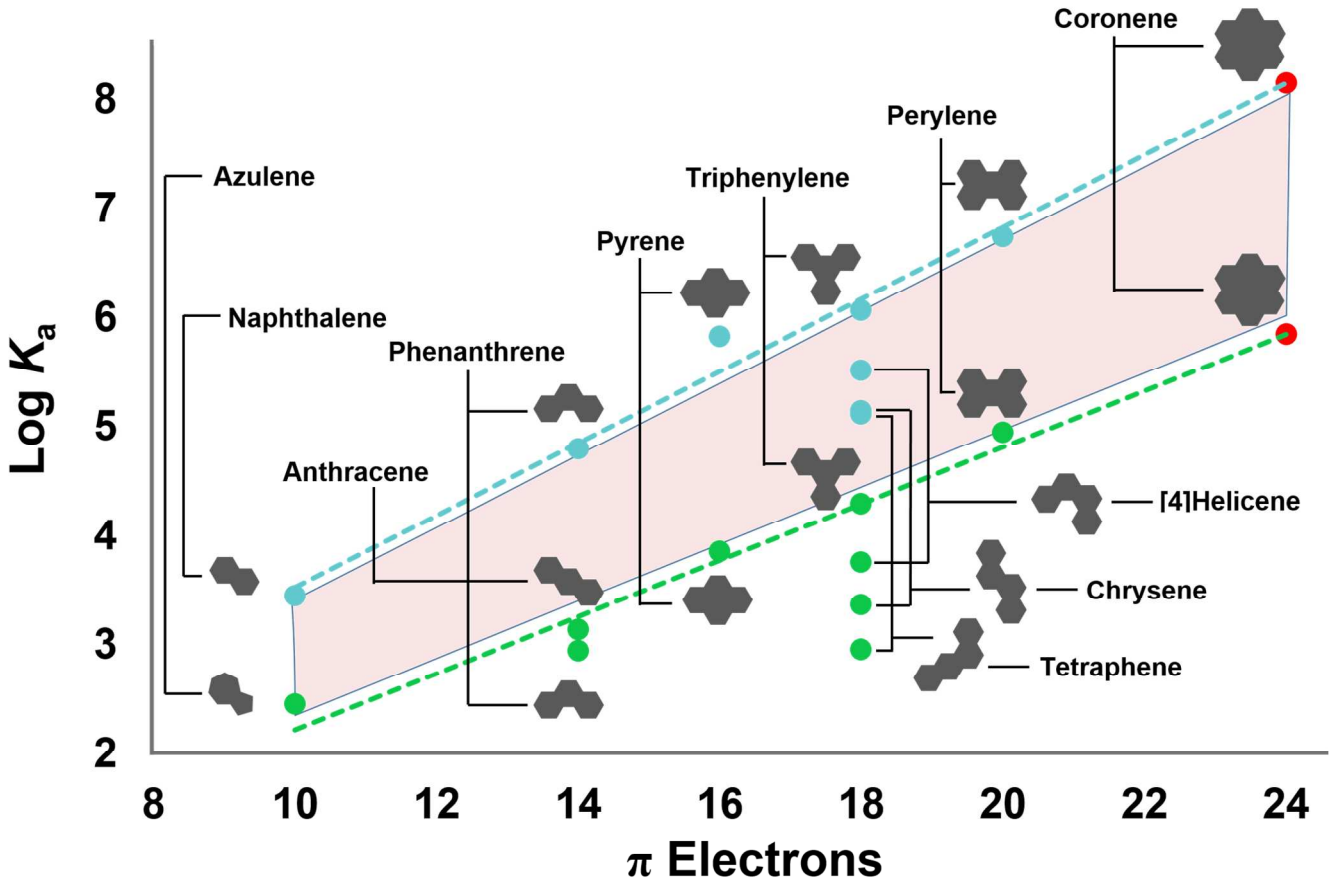

Figure 8. A plot of the association constants in MeCN between **ExCage**•6PF_6 (cyan line) and **ExBox**•4PF_6 (green line) on a logarithmic scale versus the number of π-electrons present in the selected PAHs, plus coronene (the red dot, resulting from a linear regression) for which there is no experimentally derived K_a value. The gap along the y-axis (beige) between the association constants of PAHs with **ExBox**•4PF_6 and **ExCage**•6PF_6 provides a quantitative visualization of the macrobicyclic effect. Adapted with permission from references 31 and 34. Copyright (2013 and 2014) American Chemical Society.

($\Delta G_a^{\ddagger}$), respectively, in describing host–guest complexes. The free energy of activation for decomplexation ($\Delta G_d^{\ddagger}$), therefore, is equal to the combined values of the intrinsic and constrictive binding — $\Delta G_a^{\ddagger} + \Delta G^0 = \Delta G_d^{\ddagger}$. Pyrene and coronene were identified as "small" and "large" substrates, respectively, in an exploration of the kinetics into and out of the binding cavity. The intrinsic binding was measured by ITC at 25 °C in DMF, resulting in a free energy of complexation equal to −6.88 and estimated at −8.52 kcal mol^{-1}, respectively. The barriers to

decomplexation, which were obtained in DMF-d_7 by dynamic ^{1}H NMR spectroscopy undergo a significant increase from 13.6 up to >18.7 kcal mol^{-1}, resulting in constrictive bindings of 6.7 and >8 kcal mol^{-1}, respectively. The effect of constrictive binding was confirmed by employing rapid-injection ^{1}H NMR spectroscopy in DMF-d_7 at –55 °C. This technique revealed a difference

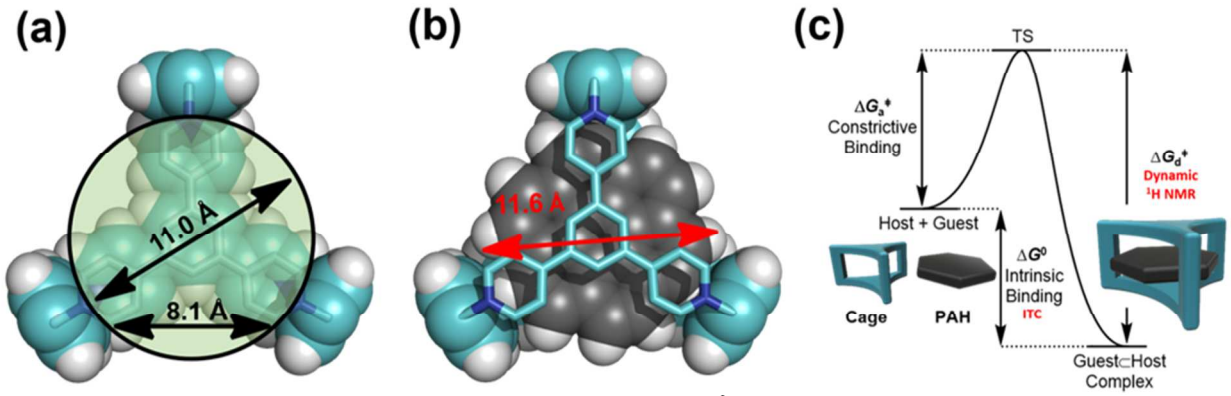

Figure 9. The **(a)** dimensions of the internal binding cavity of **ExCage**$^{6+}$ and aperture leading to it. A large guest such as coronene **(b)** will experience a barrier to complexation. This association barrier can be obtained **(c)** indirectly by subtracting the intrinsic binding from the barrier to dissociation. Adapted with permission from reference 34. Copyright (2014) American Chemical Society.

in the rate of complexation on the order of seconds for pyrene versus tens of minutes for coronene. In the case of **ExCage**$^{6+}$, while the smaller PAHs form complexes faster than the larger ones, the larger PAHs form stronger complexes than the smaller ones.

■ ExBox^{4+} as Part of a MIM

Following in the footsteps of **Ex^{0}Box**$^{4+}$ as a component of MIMs[25] — and more specifically bistable MIMs[50] — **ExBox**$^{4+}$ has been incorporated[51] into an acid- and redox-switchable [2]catenane where the recognition site in the ring mechanically interlocking the cyclophane consists of an unmetallated porphyrin. The synthesis of the **ExBox**$^{4+}$–porphyrin [2]catenane begins with the threading of the polyethylene glycol-functionalized porphyrin through the cavity of **ExBox**$^{4+}$ prior to ring-closing metathesis of the terminal olefins in the porphyrin thread, yielding 17% of the [2]catenane where **ExBox**$^{4+}$ resides on the porphyrin unit in the ground-state co-conformation (GSCC). The GSCC can be disrupted (**Figure 10**) either through the addition of

acid or by redox chemistry, thereby generating similar metastable state co-conformations (MSCC), albeit with different electronic configurations. The acid-induced switching mechanism can be triggered by the addition of trifluoroacetic acid, where the porphyrin ring becomes protonated, and drives the tetracationic **ExBox**$^{4+}$ away from encircling the porphyrin unit as a consequence of Coulombic repulsion and the loss of planarity[52] of the porphyrin ring. The reversibility of this acid-induced mechanism was vetted by treating the protonated form of the [2]catenane with cross-linked poly-4-vinylpyridine, which deprotonates the porphyrin unit and returns the MIM to its GSCC. This process was reproduced on the same sample for three cycles

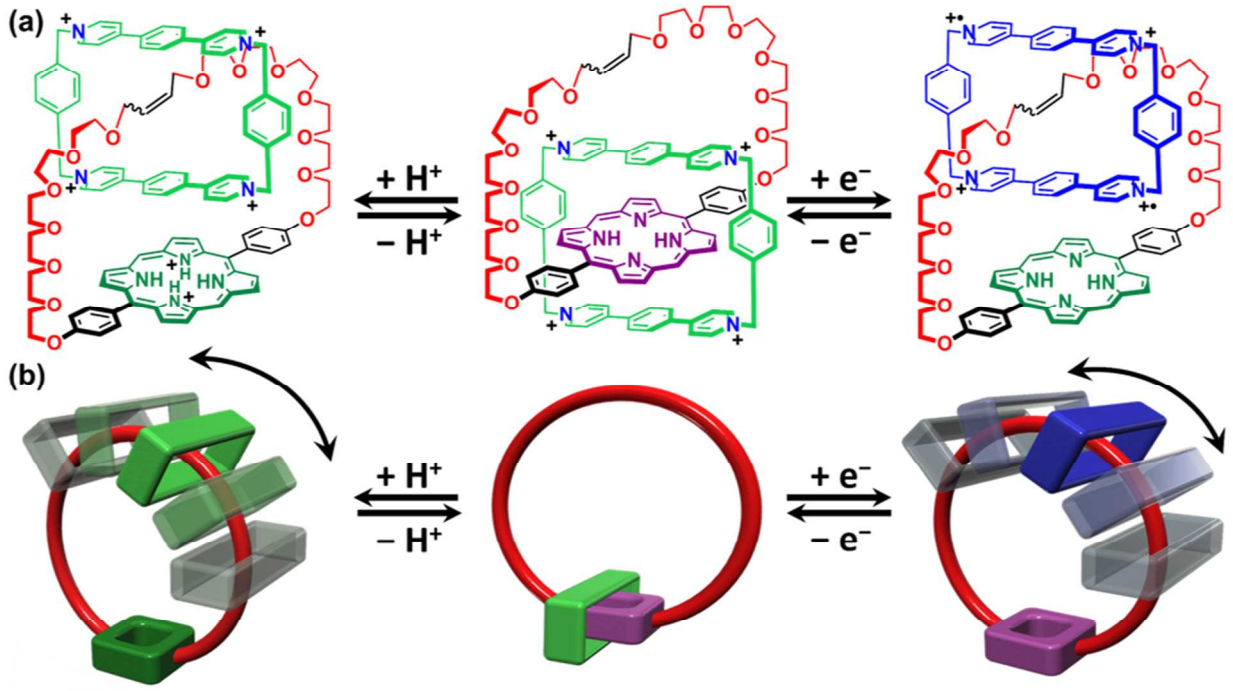

Figure 10. The molecular formulas **(a)** and graphical representations **(b)** of the [2]catenane in its ground-state co-conformation (center), the pH-based switching (left) and electrochemical removal (right) of the donor–acceptor recognition between **ExBox**$^{4+}$ and the porphyrin station. Adapted with permission from reference 51. Copyright (2014) The Royal Society of Chemistry.

before any decomposition could be detected. Additionally, electrochemical reduction of **ExBox**$^{4+}$ diminishes its affinity for interacting with the porphyrin unit, yielding another way of inducing switching in this [2]catenane. Since the cavity of **ExBox**$^{4+}$ and the series of **Ex^{n}Box**$^{4+}$ receptors accommodate a large number of diverse substrates, more switchable [2]catenanes are

conceivable.

■ PHOTOPHYSICAL PROPERTIES

The fact that the **Ex^{n}Box^{4+}** family of cyclophanes is capable of forming complexes with larger, π-electron-rich substrates that absorb light in the visible region, in combination with its ability to accept multiple electrons, bodes well for its integration into reaction centers in artificial photosynthetic systems.[53,54] Since perylene functions[55,56] as a typical chromophore in these artificial systems, we chose to investigate[57] its ability to undergo through-space intermolecular photo-induced electron transfer to **ExBox^{4+}** upon excitation of the substrate in perylene⊂**ExBox^{4+}**. Femtosecond transient absorption (fsTA) experiments show that, following photo-excitation of a dilute solution of perylene⊂**ExBox^{4+}** in MeCN, the signature radical absorption bands for the reduced *p*-phenylene-bridged viologen unit were observed at 1007 and 1175 nm, indicative of electron transfer from the excited state of the substrate — namely ^{1*}Per — to one of the extended viologen units of the cyclophane. The forward electron transfer (FET) process occurs in less than 250 fs — presumably on account of the strength of the noncovalent bonding interactions and the close proximity of each component comprising the inclusion complex — while the back electron transfer (BET) from **ExBox^{3+}** to Per$^{+\bullet}$ happens in 40 ps. Additionally, energy transfer between functionalized perylenediimides and **ExBox^{4+}** was explored in water, resulting in complexes that are highly selective for sensing melatonin.[58] Alongside using **ExBox^{4+}** as part of a complex for potential *inter*molecular electron transfer in artificial photosynthetic systems, we have also demonstrated[59,60] that photo-induced *intra*molecular electron transfer is possible with just **Ex^{n}Box^{4+}** alone. For n = 0 and 1, direct UV excitation of the cyclophane produces absorption bands which correspond well to previously reported[61] spectra for the reduced extended viologen monoradical oxidation state, indicating a

rapid FET process. However, for the longer n = 2 and 3 cyclophanes, the electronic coupling between the *p*-phenylene and the Ex^{n}BIPY units is reduced and the decay is dominated by fluorescence. Representative fsTA spectra are shown in **Figure 11**. These two examples of *inter-*

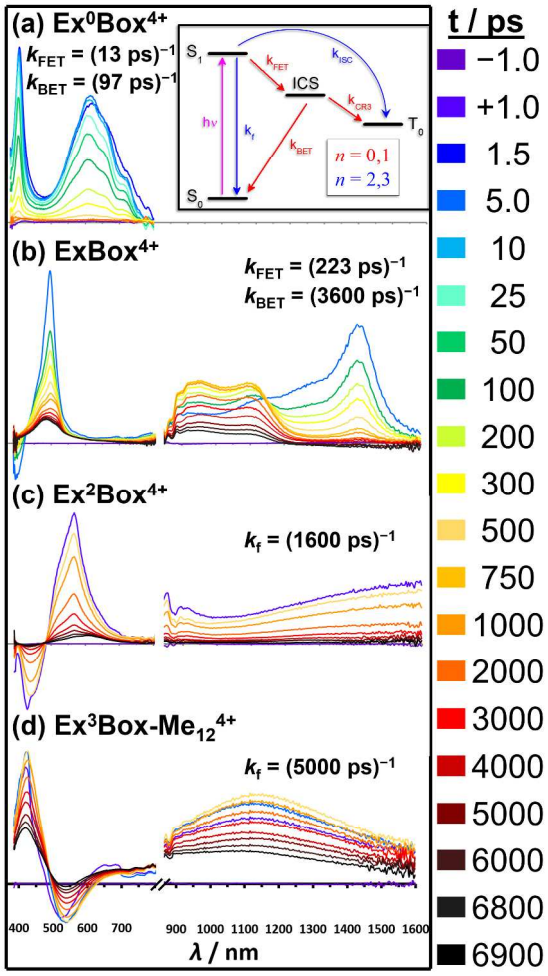

Figure 11. Femtosecond transient absorption spectra of **Ex^{0}Box^{4+}** following ultraviolet excitation at 275 nm for (a), and 330 nm for (b–d). The rate of FET decreases from k_{FET} = 13 ps^{-1} in **Ex^{0}Box^{4+}** to k_{FET} = 223 ps^{-1} in **ExBox^{4+}**. The fluorescence lifetimes similarly increase from **Ex^{2}Box^{4+}** to **Ex^{3}Box^{4+}**. For n = 1–3, some of the population decays to a low-lying triplet state.

and *intra*molecular photo-induced electron transfer further demonstrate the versatility and sophistication associated with the **Ex^{n}Box^{4+}** cyclophanes, while the larger boxes show how the spacers themselves influence the excited state decay of the macrocycle. Moreover, these preliminary photophysical explorations set the stage for further investigations into the potential

for multi-electron charge accumulation in doubly photo-excited **Ex*n*Box**$^{4+}$ inclusion complexes through orthogonal ET pathways.

■ PARTING THOUGHTS

Structure–activity relationships (SARs) are pursued in depth in the field of medicinal chemistry to explore the effect that modest structural modifications to the substrate have on the affinity and activity of a receptor. In our recent research on cationic cyclophanes, we have explored how structural modifications to the receptor, not only change the affinity profile for substrate molecules, but — in common with enzymes — can also change the properties of the receptor completely. It is no surprise then, when viewed as an analogue of a SAR, where slight variations in enzyme structure can lead to major differences in substrate specificity, that there is large variation in the performance and applications for different variations of **Ex*n*Box**$_m^{4+}$ cyclophanes. This class of receptor invites a growing landscape of potential applications related to, *e.g.*, (i) binding properties, (ii) sequestration and extraction, (iii) thermodynamic versus kinetic complexation, (iv) mechanically interlocked molecules, (v) catalysis, (vi) artificial photosystems, and (vii) molecular electronics. Thus, with a facile, modular synthesis utilizing TBAI and a wealth of areas yet to be explored, it is hoped that this Account will serve as a call to action for the continued exploration of this class of purpose-designed receptor.

■AUTHOR INFORMATION

Corresponding Author

*Professor J. Fraser Stoddart. Tel: (+1)-847-491-3793. Fax: (+1)-847-491-1009. Email: stoddart@northwestern.edu.

*Professor Michael R. Wasielewski. Tel: (+1)-847-467-1423. Email: m-wasielewski@northwestern.edu

Notes

The authors declare no competing financial interest.

Biographies

Edward J. Dale received B.A. in Chemistry and Biochemistry from Knox College in 2010. He is currently working towards his Ph.D. at Northwestern University under the supervision of Professors Fraser Stoddart and Samuel Stupp. His research involves the host–guest chemistry of cationic cyclophanes and the self-assembly of artificial muscle-like molecules.

Nicolaas A. Vermeulen received his Ph.D. at the University of Illinois at Urbana-Champaign under Professor Christina White developing late-stage C-H oxidation methodology before joining Professor Fraser Stoddart at Northwestern University as a postdoctoral fellow. He is currently a postdoctoral researcher with Professors Joseph T. Hupp and Omar. K. Farha developing new applications for robust Metal-Organic Frameworks.

Michal Juríček received B.Sc. and M.Sc. Degrees from Comenius University in Bratislava and Ph.D. Degree from Radboud University Nijmegen before he joined the group of Professor Fraser Stoddart at Northwestern University as a postdoctoral fellow. He currently leads an independent research group at University of Basel, where he investigates polycyclic hydrocarbons with delocalized spin density.

Jonathan C. Barnes obtained BS/MS degrees from the University of Kentucky and his PhD at Northwestern University under the supervision of Professor Fraser Stoddart, where he focused on molecular receptors for the sequestration of environmental pollutants and utilizing the radical molecular recognition of viologens. Jonathan is currently a Howard Hughes Medical Institute postdoctoral fellow of the Life Sciences Research Foundation at the Massachusetts Institute of Technology with Professor Jeremiah Johnson, working on methodologies for the synthesis of sequence-defined polymers, as well as the development of combination chemotherapeutics.

Ryan M. Young obtained his B.S. in Chemistry at the University of California, Los Angeles in 2006. He then studied anion dynamics using time-resolved photoelectron imaging at the University of California, Berkeley in the group of Daniel Neumark, receiving his Ph.D. in 2011. From there, he joined Michael Wasielewki's group at Northwestern University as a Camille and Henry Dreyfus Environmental Chemistry Postdoctoral Fellow, and is currently a Research Assistant Professor at Northwestern University.

Michael R. Wasielewski received his B.S. and Ph.D. degrees from the University of Chicago. He is currently the Clare Hamilton Hall Professor of Chemistry at Northwestern University. His research focuses on light-driven processes in molecules and materials, artificial photosynthesis, molecular electronics, and molecular spintronics.

J. Fraser Stoddart received B.Sc., Ph.D., and D.Sc. Degrees from the University of Edinburgh. He currently holds a Board of Trustees Professorship in the Department of Chemistry at Northwestern University. His research in molecular nanotechnology involves the synthesis and self-assembly of supramolecular and mechanically interlocked compounds and their applications in new materials and technologies.

■ ACKNOWLEDGEMENTS

We thank the Joint Center of Excellence in Integrated Nano-Systems (JCIN) at King Abdul-Aziz City for Science and Tecnology (KACST) and Northwestern University (NU) for supporting this research. This research was supported by the Chemical Sciences, Geosciences, and Biosciences Division, Office of Basic Energy Sciences, DOE, under grant no. DE-FG02-99ER14999 (M.R.W.) E.J.D. is supported by a Graduate Research Fellowship from the National Science Foundation and gratefully acknowledges support from the Ryan Fellowship and the NU International Institute for Nanotechnology. M.J. gratefully acknowledges The Netherlands Organisation for Scientific Research (NWO) and the Marie Curie Cofund Action (Rubicon Fellowship) and the Swiss National Science Foundation (SNF, PZ00P2_148043) for financial support.

■ REFERENCES

(1) Pedersen, C. J. Macrocyclic Polyethers for Complexing Metals. *Aldrichimica Acta* **1971**, *4*, 1–4.
(2) Pedersen, C. J. Cyclic Polyethers and Their Complexes with Metal Salts. *J. Am. Chem. Soc.* **1967**, *89*, 2495–2496.
(3) Pedersen, C. J. Cyclic Polyethers and Their Complexes with Metal Salts. *J. Am. Chem. Soc.* **1967**, *89*, 7017–7036.
(4) Dietrich, B.; Lehn, J.-M.; Sauvage, J.-P. Diaza-Polyoxa-Macrocycles et Macrobicycles. *Tetrahedron Lett.* **1969**, *10*, 2885–2888.
(5) Dietrich, B.; Lehn, J.-M.; Sauvage, J.-P. Les Cryptates. *Tetrahedron Lett.* **1969**, *10*, 2889–2892.
(6) Kyba, E. P.; Helgeson, R. C.; Madan, K.; Gokel, G. W.; Tarnowski, T. L.; Moore, S. S.; Cram, D. J. Host-Guest Complexation. 1. Concept and Illustration. *J. Am. Chem. Soc.* **1977**, *99*, 2564–2571.
(7) Fischer, E. Einfluss Der Configuration Auf Die Wirkung Der Enzyme. *Berichte der Dtsch. Chem.* **1894**, *27*, 2985–2993.
(8) Lehn, J.-M. *Supramolecular Chemistry: Concepts and Perspectives*; Wiley-VCH: Weinheim, Germany, 1995.
(9) Cram, D. J.; Cram, J. M. *Container Molecules and Their Guests*; Stoddart, J. F., Ed.; Royal Society of Chemistry: Cambridge, 1997.
(10) Stoddart, J. F. A Century of Cyclodextrins. *Carbohydr. Res.* **1989**, *192*, xii – xv.
(11) Crini, G. Review: A History of Cyclodextrins. *Chem. Rev.* **2014**, *114*, 10940–10975.

(12) Hiraoka, M.; Kaneda, T.; Kimura, E.; Kimura, K.; Koga, K.; Nakatsuji, Y.; Okahara, M.; Sasaki, S.; Shinkai, S.; Shono, T.; Tsukube, H. *Crown Ethers and Analogous Compounds*; Hiraoka, M., Ed.; Elsevier: Amsterdam, 2013.
(13) Gutsche, C. D.; Muthukrishnan, R. Calixarenes. 1. Analysis of the Product Mixtures Produced by the Base-Catalyzed Condensation of Formaldehyde with Para-Substituted Phenols. *J. Org. Chem.* **1978**, *43*, 4905–4906.
(14) Gutsche, C. D. *Calixarenes: An Introduction*; Royal Society of Chemistry: Cambridge, 2008.
(15) Freeman, W. A.; Mock, W. L.; Shih, N. Y. Cucurbituril. *J. Am. Chem. Soc.* **1981**, *103*, 7367–7368.
(16) Huang, W.-H.; Liu, S.; Isaacs, L. *Modern Supramolecular Chemistry*; Diederich, F., Stang, P. J., Tykwinski, R. R., Eds.; Wiley-VCH: Weinheim, Germany, 2008.
(17) Küster, W. Beitrage Zur Kenntnisd Des Bilirubins und Hämins. *Hoppe Seyler's Z. Physiol. Chem.* **1912**, *82*, 463–483.
(18) Barbe, J.-M.; Dini, D.; Donzello, M. P.; Ercolani, C.; Floris, B.; Guilard, R.; Hanack, M.; Harvey, P. D.; Kadish, K. M.; Nolte, R. J. M.; Rowan, A. E.; Stern, C.; Thordarson, P. *The Porphyrin Handbook*; Kadish, K. M., Smith, K. M., Guilard, R., Eds.; Academic Press: San Diego, 2003.
(19) Diederich, F. *Cyclophanes*; Stoddart, J. F., Ed.; Royal Society of Chemistry: Cambridge, 1991.
(20) *Modern Cyclophane Chemistry*; Gleiter, R.; Hopf, H., Eds.; Wiley-VCH: Weinheim, Germany, 2004.
(21) Ogoshi, T.; Kanai, S.; Fujinami, S.; Yamagishi, T.; Nakamoto, Y. Para-Bridged Symmetrical Pillar[5]arenes: Their Lewis Acid Catalyzed Synthesis and Host-Guest Property. *J. Am. Chem. Soc.* **2008**, *130*, 5022–5023.
(22) Tan, L.-L.; Yang, Y.-W. Molecular Recognition and Self-Assembly of Pillarenes. *J. Incl. Phenom. Macrocycl. Chem.* **2014**, *81*, 13–33.
(23) Bühner, M.; Geuder, W.; Gries, W.; Hünig, S.; Koch, M.; Poll, T. A Novel Type of Cationic Host Molecules with π-Acceptor Properties. *Angew. Chem. Int. Ed. Engl.* **1988**, *27*, 1553–1556.
(24) Odell, B.; Reddington, M. V.; Slawin, A. M. Z.; Spencer, N.; Stoddart, J. F.; Williams, D. J. Cyclobis(Paraquat-*p*-Phenylene). A Tetracationic Multipurpose Receptor. *Angew. Chem. Int. Ed. Engl.* **1988**, *27*, 1547–1550.
(25) Stoddart, J. F. The Chemistry of the Mechanical Bond. *Chem. Soc. Rev.* **2009**, *38*, 1802–1820.
(26) Ashton, P. R.; Brown, C. L.; Chrystal, E. J. T.; Goodnow, T. T.; Kaifer, A. E.; Parry, K. P.; Philp, D.; Slawin, A. M. Z.; Spencer, N.; Stoddart, J. F.; Williams, D. J. The Self-Assembly of a Highly Ordered [2]Catenane. *J. Chem. Soc. Chem. Commun.* **1991**, 634–639.
(27) Philp, D.; Slawin, A. M. Z.; Spencer, N.; Stoddart, J. F.; Williams, D. J. The Complexation of Tetrathiafulvalene by Cyclobis(Paraquat-*p*-Phenylene). *J. Chem. Soc. Chem. Commun.* **1991**, 1584–1586.
(28) Trabolsi, A.; Khashab, N.; Fahrenbach, A. C.; Friedman, D. C.; Colvin, M. T.; Cotí, K. K.; Benítez, D.; Tkatchouk, E.; Olsen, J.-C.; Belowich, M. E.; Carmielli, R.; Khatib, H. A.; Goddard, W. A.; Wasielewski, M. R.; Stoddart, J. F. Radically Enhanced Molecular Recognition. *Nat. Chem.* **2010**, *2*, 42–49.

(29) Miljanić, O. Š.; Stoddart, J. F. Dynamic Donor–Acceptor [2]Catenanes. *Proc. Natl. Acad. Sci. U. S. A.* **2007**, *104*, 12966–12970.
(30) Barnes, J. C.; Juríček, M.; Vermeulen, N. A.; Dale, E. J.; Stoddart, J. F. Synthesis of Ex^{n}Box Cyclophanes. *J. Org. Chem.* **2013**, *78*, 11962–11969.
(31) Barnes, J. C.; Juríček, M.; Strutt, N. L.; Frasconi, M.; Sampath, S.; Giesener, M. A.; McGrier, P. L.; Bruns, C. J.; Stern, C. L.; Sarjeant, A. A.; Stoddart, J. F. ExBox: A Polycyclic Aromatic Hydrocarbon Scavenger. *J. Am. Chem. Soc.* **2013**, *135*, 183–192.
(32) Juríček, M.; Barnes, J. C.; Dale, E. J.; Liu, W.-G.; Strutt, N. L.; Bruns, C. J.; Vermeulen, N. A.; Ghooray, K. C.; Sarjeant, A. A.; Stern, C. L.; Botros, Y. Y.; Goddard, W. A.; Stoddart, J. F. Ex^{2}Box: Interdependent Modes of Binding in a Two-Nanometer-Long Synthetic Receptor. *J. Am. Chem. Soc.* **2013**, *135*, 12736–12746.
(33) Barnes, J. C.; Dale, E. J.; Prokofjevs, A.; Narayanan, A.; Gibbs-Hall, I. C.; Juríček, M.; Stern, C. L.; Sarjeant, A. A.; Botros, Y. Y.; Stupp, S. I.; Stoddart, J. F. Semiconducting Single Crystals Comprising Segregated Arrays of Complexes of C_{60}. *J. Am. Chem. Soc.* **2015**, *137*, 2392–2399.
(34) Dale, E. J.; Vermeulen, N. A.; Thomas, A. A.; Barnes, J. C.; Juríček, M.; Blackburn, A. K.; Strutt, N. L.; Sarjeant, A. A.; Stern, C. L.; Denmark, S. E.; Stoddart, J. F. ExCage. *J. Am. Chem. Soc.* **2014**, *136*, 10669–10682.
(35) Hafezi, N.; Holcroft, J. M.; Hartlieb, K. J.; Dale, E. J.; Vermeulen, N. A.; Stern, C. L.; Sarjeant, A. A.; Stoddart, J. F. Modulating the Binding of Polycyclic Aromatic Hydrocarbons inside a Hexacationic Cage by Anion-π Interactions. *Angew. Chem. Int. Ed. Engl.* **2015**, *54*, 456–461.
(36) Anderson, S.; Anderson, H. L.; Sanders, J. K. M. Expanding Roles for Templates in Synthesis. *Acc. Chem. Res.* **1993**, *26*, 469–475.
(37) *Templated Organic Synthesis*; Diederich, F., Stang, P. J., Eds.; Wiley-VCH: Weinheim, Germany, 1999.
(38) Bachrach, S. M. DFT Study of the ExBox·Aromatic Hydrocarbon Host-Guest Complex. *J. Phys. Chem. A* **2013**, *117*, 8484–8491.
(39) Bachrach, S. M.; Andrews, A. E. All-Carbon, Neutral Analogue of ExBox^{4+}: A DFT Study of Polycyclic Aromatic Hydrocarbon Binding. *J. Phys. Chem. A* **2014**, *118*, 6104–6111.
(40) Antony, J.; Sure, R.; Grimme, S. Using Dispersion-Corrected Density Functional Theory to Understand Supramolecular Binding Thermodynamics. *Chem. Commun.* **2015**, *51*, 1764–1774.
(41) Seiders, T. J.; Baldridge, K. K.; Grube, G. H.; Siegel, J. S. Structure/Energy Correlation of Bowl Depth and Inversion Barrier in Corannulene Derivatives: Combined Experimental and Quantum Mechanical Analysis. *J. Am. Chem. Soc.* **2001**, *123*, 517–525.
(42) Juríček, M.; Strutt, N. L.; Barnes, J. C.; Butterfield, A. M.; Dale, E. J.; Baldridge, K. K.; Stoddart, J. F.; Siegel, J. S. Induced-Fit Catalysis of Corannulene Bowl-to-Bowl Inversion. *Nat. Chem.* **2014**, *6*, 222–228.
(43) Koshland, D. E. Application of a Theory of Enzyme Specificity to Protein Synthesis. *Proc. Natl. Acad. Sci. U. S. A.* **1958**, *44*, 98–104.
(44) Marc Veen, E.; Feringa, B. L.; Postma, P. M.; Jonkman, H. T.; Spek, A. L. Solid State Organisation of C_{60} by Inclusion Crystallisation with Triptycenes. *Chem. Commun.* **1999**, 1709–1710.
(45) Atwood, J. L.; Barbour, L. J.; Raston, C. L. Supramolecular Organization of C_{60} into

Linear Columns of Five-Fold, Z-Shaped Strands. *Cryst. Growth Des.* **2002**, *2*, 3–6.
(46) Xia, J.; Bacon, J. W.; Jasti, R. Gram-Scale Synthesis and Crystal Structures of [8]- and [10]CPP, and the Solid-State Structure of C_{60}@[10]CPP. *Chem. Sci.* **2012**, *3*, 3018.
(47) Diederich, F.; Gómez-López, M. Supramolecular Fullerene Chemistry. *Chem. Soc. Rev.* **1999**, *28*, 263–277.
(48) Mecozzi, S.; Rebek, Jr., J. The 55 % Solution: A Formula for Molecular Recognition in the Liquid State. *Chem. Eur. J.* **1998**, *4*, 1016–1022.
(49) Cram, D. J.; Blanda, M. T.; Paek, K.; Knobler, C. B. Constrictive and Intrinsic Binding in a Hemicarcerand Containing Four Portals. *J. Am. Chem. Soc.* **1992**, *114*, 7765–7773.
(50) Saha, S.; Stoddart, J. F. Molecular Motors and Muscles. In *Functional Organic Materials*; Wiley: Weinheim, Germany, 2007.
(51) Juríček, M.; Barnes, J. C.; Strutt, N. L.; Vermeulen, N. A.; Ghooray, K. C.; Dale, E. J.; McGonigal, P. R.; Blackburn, A. K.; Avestro, A.-J.; Stoddart, J. F. An ExBox [2]Catenane. *Chem. Sci.* **2014**, *5*, 2724–2371.
(52) Stone, A.; Fleischer, E. B. The Molecular and Crystal Structure of Porphyrin Diacids. *J. Am. Chem. Soc.* **1968**, *90*, 2735–2748.
(53) Wasielewski, M. R. Photoinduced Electron Transfer in Supramolecular Systems for Artificial Photosynthesis. *Chem. Rev.* **1992**, *92*, 435–461.
(54) Gust, D.; Moore, T. A.; Moore, A. L. Molecular Mimicry of Photosynthetic Energy and Electron Transfer. *Acc. Chem. Res.* **1993**, *26*, 198–205.
(55) Davis, W. B.; Ratner, M. A.; Wasielewski, M. R. Dependence of Electron Transfer Dynamics in Wire-like Bridge Molecules on Donor–bridge Energetics and Electronic Interactions. *Chem. Phys.* **2002**, *281*, 333–346.
(56) Brown, K. E.; Veldkamp, B. S.; Co, D. T.; Wasielewski, M. R. Vibrational Dynamics of a Perylene-Perylenediimide Donor-Acceptor Dyad Probed with Femtosecond Stimulated Raman Spectroscopy. *J. Phys. Chem. Lett.* **2012**, *3*, 2362–2366.
(57) Young, R. M.; Dyar, S. M.; Barnes, J. C.; Juríček, M.; Stoddart, J. F.; Co, D. T.; Wasielewski, M. R. Ultrafast Conformational Dynamics of Electron Transfer in $ExBox^{4+}$⊂Perylene. *J. Phys. Chem. A* **2013**, *117*, 12438–12448.
(58) Ryan, S. T. J.; Del Barrio, J.; Ghosh, I.; Biedermann, F.; Lazar, A. I.; Lan, Y.; Coulston, R. J.; Nau, W. M.; Scherman, O. A. Efficient Host-Guest Energy Transfer in Polycationic Cyclophane-Perylene Diimide Complexes in Water. *J. Am. Chem. Soc.* **2014**, *136*, 9053–9060.
(59) Dyar, S. M.; Barnes, J. C.; Juríček, M.; Stoddart, J. F.; Co, D. T.; Young, R. M.; Wasielewski, M. R. Electron Transfer and Multi-Electron Accumulation in $ExBox^{4+}$. *Angew. Chemie Int. Ed.* **2014**, *126*, 5475–5479.
(60) Barnes, J. C.; Frasconi, M.; Young, R. M.; Khdary, N. H.; Liu, W.-G.; Dyar, S. M.; McGonigal, P. R.; Gibbs-Hall, I. C.; Diercks, C. S.; Sarjeant, A. A.; Stern, C. L.; Goddard, W. A.; Wasielewski, M. R.; Stoddart, J. F. Solid-State Characterization and Photoinduced Intramolecular Electron Transfer in a Nanoconfined Octacationic Homo[2]Catenane. *J. Am. Chem. Soc.* **2014**, *136*, 10569–10572.
(61) Barnes, J. C.; Fahrenbach, A. C.; Dyar, S. M.; Frasconi, M.; Giesener, M. A.; Zhu, Z.; Liu, Z.; Hartlieb, K. J.; Carmieli, R.; Wasielewski, M. R.; Stoddart, J. F. Mechanically Induced Intramolecular Electron Transfer in a Mixed-Valence Molecular Shuttle. *Proc. Natl. Acad. Sci. U. S. A.* **2012**, *109*, 11546–11551.